*Proceedings World Geothermal Congress 2000*
*Kyushu - Tohoku, Japan, May 28 - June 10, 2000*

# APPLICATION OF CHEMICAL AND WELLBORE MODELLING TO THE CORROSION AND SCALING PROPERTIES OF OHAAKI DEEP WELLS

Stephen White[*], Keith Lichti[+] and Lew Bacon[#]
[*]Applied Mathematics, Industrial Research Limited, PO Box 31-310, Lower Hutt, New Zealand
[+]Materials Performance Technologies, PO Box 31-310, Lower Hutt, New Zealand
[#]Contact Energy, Private Bag 2001, Taupo, New Zealand

**Key words: Chemical, Wellbore, Geothermal, Modelling, Potential-pH, Corrosion, Scaling, Ohaaki, Mahanagdong**

## ABSTRACT

Thermodynamic models are used to calculate the chemistry of the inflow into existing deep wells from measured surface chemistry and enthalpy. This information, together with wellbore simulation, allows the calculation of chemical conditions throughout the wellbore. Estimates of the chemistry are incorporated into predictive phase-stability models of protective corrosion products and mineral scales. These models assist in defining the risk of corrosion and scaling in the existing deep wells. Ohaaki deep wells have produced waters having a similar chemistry to those in the shallow reservoir. This New Zealand experience can be contrasted with occasional acid fluids being experienced in other shallow geothermal fields and more acid fluids being encountered in deep wells in other fields.

## 1. INTRODUCTION

The major economic risk in the development of a geothermal reservoir is the failure of a well to produce usable geothermal fluid. Wells may fail to penetrate permeability that supports viable production, and corrosion and scaling may impact long-term productive capacity. These issues become more important as geothermal development taps the deeper geothermal resource. Not only is the investment in the well greater but the possibility of encountering poor permeability and/or low pH fluids is also increased.

The aim of this paper is to consider computer modelling techniques that allow us to determine the chemistry within the wellbore of a producing geothermal well. Once this chemistry is known it is possible to compare thermodynamic predictions of the corrosion mechanisms with other well characterised systems and therefore to estimate likely corrosion rates for the wellbore and also what scales may form. The techniques described here also allow the effect of process chemistry changes on corrosion and scaling to be calculated.

Some of the corrosion aspects of this problem have been considered by Lichti *et al*. (1998) and Lichti *et al*. (1997). Moller *et al*. (1998) have considered chemical modelling of scaling from geothermal fluid.

## 2. DATA REQUIREMENTS

Several steps are involved in determining the chemistry in a flowing well.

Firstly we must know the chemical composition of the produced fluid. This is generally obtained from analysis of separated water and gas contained in the steam. These may be combined to give the composition of the reservoir fluid at the production depth (see, for example, Reed 1981).

Secondly we must know the physical and thermodynamic conditions within the wellbore (pressure, temperature, saturation and liquid and gas velocities). These data may be calculated using a wellbore simulator such as GWELL (Aunzo *et al*. 1991) providing that the production characteristics of the well are known.

## 3. MATHEMATICAL AND CHEMICAL DETAILS

We describe the chemistry of the wellbore in terms of the total concentration of a number of primary or basis species (see Bethke, 1996 for a discussion of this approach to chemical equilibrium calculation). Lichtner (1985) referred to these concentrations as generalised concentrations. The following example outlines the concept of generalised concentrations.

Consider the system:

$$\begin{aligned} &CO_2(\text{gas}) \leftrightarrow H^+ + HCO_3^- - H_2O \\ &H_2CO_3 \leftrightarrow H^+ + HCO_3^- \\ &CO_3^= \leftrightarrow HCO_3^- - H^+ \\ &CaCO_3(\text{solid}) \leftrightarrow Ca^+ + HCO_3^- - H^+ \end{aligned} \tag{1}$$

The chemistry associated with the reaction of $CO_2$ gas and solid calcite is written in terms of the basis species $Ca^+$, $HCO_3^-$, $H_2O$ and $H^+$. These reactions can be represented by a stoichiometric matrix:

$$\begin{array}{c} \\ H_2O \\ H^+ \\ HCO_3^- \\ Ca^+ \\ CO_2(\text{gas}) \\ H_2CO_3 \\ CO_3^= \\ CaCO_3 \end{array} \begin{array}{c} \begin{array}{cccc} CO_2(\text{gas}) & H_2CO_3 & CO_3^= & \text{Calcite} \end{array} \\ \left(\begin{array}{cccc} -1 & 0 & 0 & 0 \\ 1 & 1 & -1 & -1 \\ 1 & 1 & 1 & 1 \\ 0 & 0 & 0 & 1 \\ \hline -1 & 0 & 0 & 0 \\ 0 & -1 & 0 & 0 \\ 0 & 0 & -1 & 0 \\ 0 & 0 & 0 & -1 \end{array}\right. \end{array} \begin{array}{l} \\ \\ \\ \\ \text{Primary Species} \\ \\ \text{Secondary Species} \\ \\ \end{array} \tag{2}$$

Using the stoichiometric matrix we can define the generalised concentration $\Psi_i$ of any basis species $C_i$ as:

$$\Psi_i = C_i + \sum_j S_{ij} C_j \tag{3}$$

where $C_i$ is the concentration of basis species $i$, $C_j$ is the concentration of secondary species $j$ and $S_{ij}$ is the stoichiometric coefficient giving the number of moles of primary species $i$ in secondary species $j$.

The concentrations of the chemical species in Equation (1) are governed by the conditions of chemical equilibrium which may be written in terms of the coefficients of the stoichiometric matrix as:

$$\prod_i [C_i]^{S_{ij}} = K_j \tag{4}$$

where $[C_i]$ is the activity of species $i$ and $K_j$ the equilibrium coefficient for reaction $j$.

Note that because we have $CO_2$ gas present we have a two-phase system and the primary and secondary species concentrations $C_i$, $C_j$ must be interpreted in this light i.e. they represent the concentrations in terms of the two-phase mixture, not the more normal liquid phase concentrations. Equation (3) may be rewritten as:

$$\Psi_i = C_i S_l + \left( \sum_{j=\text{liquid}} S_{ij} C_j \right) S_l + \left( \sum_{j=\text{gas}} S_{ij} C_j \right) (1 - S_l) \qquad (5)$$

where $S_l$ is the liquid saturation of the two-phase mixture, $C_i$ is now the concentration of primary species $i$ in the liquid phase and $C_j$ is the concentration of secondary species $j$ in either the liquid or gas phase. $\Psi_j$ is still the generalised concentration of basis species $i$ in the two-phase mixture. At this stage it is convenient to ignore the solid phase.

If we consider flow in a wellbore, in general we will have both liquid and vapour phases present and these will move at different velocities $V_\lambda$ and $V_g$.

The flow of the basis species within the well is governed by the conservation equation:

$$\frac{\partial \psi_i}{\partial t} = \frac{\partial \Omega_i}{\partial z} \quad i = 1, 2\text{K} \;\; \text{N}_\text{p} \qquad (6)$$

where $\Psi_i$ is the generalised concentration defined in Equation (5), $N_p$ the number of primary species and $\Omega_i$ is the generalised flux defined by

$$\Omega_i = J_i + \sum_{\text{j=liquid}} S_{ij} J_j + \sum_{\text{j=gas}} S_{ij} J_j$$

The summations are understood to be over the liquid and gaseous secondary species.

$J_i$, $J_j$ (liquid) and $J_j$ (gas) are defined as:

$$\begin{aligned} J_i &= \rho_\lambda S_\lambda V_\lambda C_i \\ J_j\ (\text{liquid}) &= \rho_\lambda S_\lambda V_\lambda C_j \\ J_j\ (\text{gas}) &= \rho_g (1 - S_\lambda) V_g C_j \end{aligned} \qquad (7)$$

where $\rho_i$ is the density, $V_i$ the velocity of phase $i$, $C_i$ the concentration of primary species $i$ and $C_j$ the concentration of secondary species $j$. Providing the wellbore is in a state of steady flow the flux of primary species must be constant throughout the well i.e:

$$\Omega_i = \text{constant} \qquad (8)$$

and the constant value for each primary species is obtained from the initial chemical condition of the reservoir fluid. We can formulate the problem of calculating the chemical conditions at any point in the wellbore as:

$$\Omega - \Omega_{\text{initial}} = 0 \qquad (9)$$

where $\Omega$ is a vector of generalised fluxes at some point in the wellbore and $\Omega_{\text{initial}}$ is the vector of basis species flows into the well.

$\Omega$ is a nonlinear function of liquid and gas concentrations. The liquid and gas velocities, temperature and pressure are known from simulation of the well using a wellbore simulator.

To solve this equation we write it as:

$$R = \Omega(C^K) - \Omega_{\text{initial}}$$

where $\Omega(C^K)$ is $\Omega$ evaluated with the estimate of the primary concentration vector $C^K$ at iteration $K$. This estimate for $C^k$ may be updated using Newton's method:

$$C^{K+1} = C^K - J^{-1} R(C^K)$$

where $J$ is the Jacobian of the system $J_{ij} = \frac{\partial R_i}{\partial C_j}$. Note that calculation of the flux vector $\Omega(C^K)$ requires the solution of the two-phase equilibrium equations (4). The Jacobian is evaluated numerically. White (1996) discusses the solution of two-phase chemical equilibrium equations and we use the method given there. An alternative approach is given by Moller *et al.* (1998).

There are two approaches that may be used to take into account the effect of deposition in the wellbore (scaling). The first is to consider all possible minerals as part of the system when solving the equations of chemical equilibrium. First the system is solved assuming no minerals are present, then the most super-saturated mineral is assumed to be present and the equilibrium equations solved again. This process is repeated until the system is not super-saturated with respect to any mineral. For each mineral that is added an equilibrium equation for that mineral is included in the system. The flux of basis species in the wellbore is reduced to account for the loss of basis species from solution.

A second approach is to ignore scaling when calculating the chemical conditions in the wellbore and simply calculate what minerals are super-saturated.

We have adopted this second approach as there are a number of complicating factors in mineral deposition that are not well enough understood to be included in the modelling.

## 4. EXAMPLES

We present examples from two geothermal reservoirs. The first is from several wells recently drilled below the current production reservoir at Ohaaki located in the Taupo Volcanic Zone, New Zealand. The second example is well MG-9D located in the Mahanagdong field in the Phillipines. MG-9D has been discussed in Lichti *et al*. (1998) and is presented here as it provides an interesting contrast in geothermal fluid types.

**Tables 1** and **2** present the measured surface chemistries and **Table 3** the chemistry of a single-phase fluid assumed as the feed fluid for the modelled wells. The Ohaaki wells have excess enthalpy and produce two-phase fluid from the reservoir. This single-phase fluid of the feed, when flashed to the two-phase conditions in the wellbore, produces the correct gas and liquid chemistry for the two-phase wellbore conditions. These wells were modelled using the wellbore simulator HOLA (Aunzo *et al*. 1991). The production rates, wellhead pressures and feed point locations are given in **Table 4**.

The results of this wellbore modelling together with the procedures outlined in section 2 allowed the calculation of chemistry throughout the wellbores. In **Figure 1** we present

pH, total sulfur in the liquid phase and partial pressure of $H_2$ as functions of well depth.

## 5. SCALING POTENTIAL

**Table 5** presents a list of minerals that are super-saturated at a depth of 200 meters in each well. This table was calculated using the SOLVEQ computer program and the SOLTHERM geochemical database (Spycher and Reed 1990) to calculate the saturation indices of all minerals contained in the database. In many cases the actual minerals precipitated will depend on the kinetics of the reaction, the surface area available for deposition and perhaps other factors.

## 6. CORROSION

Potential-pH diagrams can be used to describe equilibrium corrosion reactions of pure iron in contact with corrosive liquid environments. Diagrams for the Fe-$H_2S$-$H_2O$ system having total sulfur ($SO_4^{=}$+$HS^-$+$H_2S$) with values in the range illustrated in Figure 1, and listed in Table 6, were prepared. Diagrams for the Ohaaki deep well conditions were very similar and showed little sensitivity to temperature in the 175 to 200°C range. Figure 2 represents the diagram for well BR42 at 200°C. The diagram predicts corrosion product stability as a function of pH, total S and corrosion potential. Figure 2 shows the formation of stable passive films troilite (FeS) and pyrite ($FeS_2$) and possibly magnetite ($Fe_3O_4$), on carbon steel in the neutral to alkaline pH region of the diagram at the predicted corrosion potential range. Such films can slow corrosion to low acceptable levels, however the potential-pH diagrams do not predict kinetics of corrosion reactions. Lichti *et al*. (1997) demonstrated formation of magnetite below iron sulfide films after a period of time of exposure to similar fluids derived from the Ohaaki and Kawerau shallow steam fields. The sulfide films which form block the surface from the corrosive solution and give an effective reduction in the total S at the reaction surface.

Braithwaite and Lichti (1980), Lichti *et al*. (1981) and Lichti *et. al*. (1997) further demonstrated that Ohaaki shallow well fluids having neutral to alkaline pH with water and steam chemistry similar to that of the deep wells give parabolic to logarithmic type corrosion kinetics with corrosion rates less than 0.08 mm per year. Localised attack in these environments has been observed, but again rates are generally less than 0.08 mm per year.

The deep well calculated pH of 6.9 provides neutral pH, dilute chloride waters where formation of passive films and low corrosion rates are predicted. This can be contrasted to corrosion problems reported previously, for Mahanagdong well MG-9D in the Philippines (Lichti *et al*. 1998) where the predicted chemistry gave a potential-pH diagram as shown in Figure 3.

In this instance, the acidic well fluids had a pH of about 3.5 at 200°C. The potential-pH diagram shows the predicted corrosion potential range as overlapping the $Fe^{2+}$ and iron sulfide stability areas. This suggests the fluids will probably be very corrosive, particularly, if the fluids are turbulent giving rise to erosion corrosion (Ikeuchi *et al*. 1997).

## 7. DISCUSSION AND CONCLUSIONS

Coupling of wellbore simulation to two-phase equilibrium chemical modelling allows calculation of the thermodynamic and chemical conditions within a flowing well. These may be different from those calculated using a simple, single step boiling approach. The iterative approach used gives an accurate representation of the corrosion chemistry of the water phase as it ascends the wellbore.

The model has been applied to deep wells at Ohaaki geothermal field. In this instance the deep well fluids have similar chemistry to the shallow reservoir fluids and are of neutral-pH dilute chloride type. The predicted wellbore chemistry was used to estimate scaling potential by calculation of saturation indices but these indices give no information on scaling kinetics.

More information is available for kinetics of corrosion reactions. Thermodynamic potential-pH Pourbaix diagrams for the deep well fluid chemistry predict stable passive film formation. Comparison with previous experience and research for similar fluids in this and other New Zealand geothermal fields suggests these passive films will give rise to low acceptable corrosion rates.

The more acidic geothermal well, MG-9D at Mahanagdong in the Philippines has reservoir fluids of moderate pH (around 4) but the wellbore simulation demonstrates that pH decreases as the fluid boils in the well. There is a higher iron content possibly due primarily to corrosion of the bore casing and slightly higher total S which gives iron sulfide corrosion product stability to lower pH values. Unfortunately the calculated pH is indicating that the reaction area is close to the free corrosion area where passive films are not formed. Under turbulent flow conditions the bore casing is predicted to experience unacceptable high corrosion rates.

## 8. ACKNOWLEDGEMENTS

This paper was prepared using financial support from the New Zealand Foundation for Research Science and Technology and from Contact Energy New Zealand Ltd. Data for well MG-9D was provided by Noel Selonga and E. Parrialla of PNOC EDC. We thank Warwick Kissling and Karen Garner for their careful review of the manuscript.

## REFERENCES

Aunzo, Z.P., Bjornsson, G., Bodvarsson, G.S. (1991) Wellbore Models GWELL, GWELLNACL and HOLA. Users Guide. Lawrence Berkeley National Laboratory Report LBL-31428

Bethke, C.M. (1996) Geochemical Reaction Modelling. Oxford University Press .

Braithwaite, W.R. and Lichti, K.A. (1980) Surface corrosion of metals in geothermal fluids at Broadlands (Ohaaki) New Zealand, Geothermal Scaling and Corrosion, ASTM STP 717. L.A. Casper and T.R. Pinchback, Eds, ASTM, pp 81-112.

Ikeuchi, J., Kimura, S., Kurata, Y., Pestov, I. and Sanada, S. (1997) Material damage in deep geothermal well brines, Proc. 19th New Zealand Geothermal Workshop, pp 175-180.

Lichti, K. A., White, S. P., Sanada, N. (1998) Corrosion in deep and acidic geothermal wells. *19th PNOC-EDC GeoConf*, Manila, pp 199-212.

Lichti, K. A., Swann, S. S., White, S. P., Sanada, N., Kurata, Y., Nanjo, H., Ikeuchi J. and Christenson, B. W. (1997)

Corrosion in volcanic gases, *Pro.c NEDO Int. Geo. Sym.p*, Mar. 11 and 12, Sendai, Japan, pp 154-163.

Lichti, K.A., Soylemezoglu, S. and Cunliffe, K.D. (1981) Geothermal corrosion and corrosion products, New Zealand Geothermal Workshop, pp 103-108.

Lichtner, P.C. (1985) Continium model for simultaneous chemical reactions and mass transport in hydrothermal systems, *Geochimica et Cosmochimica Acta*, 49: 779-800

Moller, N., Greenberg, J. P. and Weare, J. H. (1998) Computer modelling for geothermal systems: Predicting carbonate and silica scale formation, $CO_2$ breakout and $H_2S$ exchange, *Transport in Porous Media*, 33: 173-204.

Reed, M.H. (1981) Calculation of multicomponent chemical equilibria and reaction processes in systems involving minerals, gases and an aqueous phase. *Geochimica et Cosmochimica Acta*, 46: 513-528.

Spycher, N.F. and Reed, M.H. (1990) Users Guide for SOLVEQ: A Computer Program for Computing Aqueous-Mineral-Gas Equilibria. Department of Geological Sciences, University of Oregon report.

White, S.P., Kissling W.M., (1996) Including chloride and CO2 chemistry in large scale reservoir models. Proc 18th New Zealand Geothermal Workshop, pp. 295-300.

**Table 1**: Aqueous chemical concentrations (ppm) measured in separated water.

| Well | T | pH | $Na^+$ | $K^+$ | $Ca^{++}$ | $Cl^-$ | $SO4^{--}$ | $HCO3(tot)^-$ | $SiO_2$ |
|---|---|---|---|---|---|---|---|---|---|
| BR48 | 18 | 8.37 | 1009 | 212 | 3.6 | 1693 | 4 | 138 | 847 |
| BR49 | 23 | 8.94 | 888 | 143 | 1.35 | 1149 | 8.2 | 450 | 663 |
| BR42 | 23 | 8.36 | 1054 | 140 | 1.93 | 1595 | 6.8 | 257 | 676 |
| MG9D | 25 | 3.1 | 3117 | 950 | 82 | 6175 | 508 | - | 910 |

**Table 2:** Gas phase chemistry (mmole/100 mole of separated steam)

| Well | Enthalpy | SCP | $CO_2$ | $H_2S$ | $NH_3$ | $H_2$ | $N_2$ | $CH_4$ |
|---|---|---|---|---|---|---|---|---|
| BR48 | 1578 | .935 | 2248 | 38.2 | | | | |
| BR49 | 2134 | .890 | 1692 | 20.4 | | | | |
| BR42 | 2326 | .880 | 2731 | 24.7 | | | | |
| MG9D | 1287 | .480 | 400 | 24.3 | 0.24 | .088 | 12.7 | .95 |

**Table 3**: Calculated feedpoint chemistry (ppm) (values given are generalised concentrations, see Reed (1981) for an interpretation of negative values)

| Well | T | pH | $Na^+$ | $K^+$ | $Ca^{++}$ | $Cl^-$ | $SO4^{--}$ | $HCO3(tot)^-$ | $SiO_2$ |
|---|---|---|---|---|---|---|---|---|---|
| BR48 | 228 | 6.4 | 548 | 10 | 2.0 | 920 | 2 | 36042 | 460 |
| BR49 | 203 | 7.3 | 283 | 45 | 0.4 | 366 | -183 | 39913 | 211 |
| BR42 | 200 | 6.8 | 275 | 35 | 0.4 | 396 | 23 | 70863 | 140 |
| MG9D | 270 | 4.0 | 2175 | 662 | 57 | 4310 | 507 | 4237 | 634 |

**Table 4**: Information used in wellbore modelling.

| Well | Flow rate (kg/s) | Enthalpy (kJ/kg) | Feedpoint location (mCHF) |
|---|---|---|---|
| BR48 | 23 | 2200 | 1360,1400,1700 |
| BR49 | 11 | 2200 | 1950 |
| BR42 | 9 | 2280 | 1503 |
| MG9D | 120 | 1287 | 1679 |

**Table 5**: Minerals saturated in Ohaaki wells at 200 meters CHF under production conditions specified in Table 4

| Well | t (°C) | Mineral | log K | log Q | log Q/K |
|---|---|---|---|---|---|
| BR42 | 177 | Chalcedony | -2.37 | -2.04 | .34 |
| | | Cristobalite | -2.23 | -2.04 | .19 |
| | | Quartz | -2.50 | -2.04 | .47 |
| BR48 | 181 | Calcite | -.33 | 1.48 | 1.81 |
| | | Chalcedony | -2.35 | -1.62 | .74 |
| | | Cristobalite | -2.21 | -1.62 | .59 |
| | | Quartz | -2.48 | -1.62 | .86 |
| | | Amorphous silica | -1.87 | -1.62 | .25 |
| BR49 | 179 | Aragonite | -.09 | .37 | .45 |
| | | Calcite | -.25 | .37 | .62 |
| | | Chalcedony | -2.37 | -1.75 | .63 |
| | | Cristobalite | -2.23 | -1.75 | .48 |
| | | Graphite | -2.79 | -2.75 | .04 |
| | | Quartz | -2.50 | -1.75 | .76 |
| | | Amorphous silica | -1.88 | -1.75 | .14 |
| MG9D | 195 | Cristobalite | -2.15 | -1.62 | .53 |
| | | Pyrite | -19.86 | -17.18 | 2.67 |
| | | Amorphous silica | -1.82 | -1.62 | .21 |
| | | Minnesotaite | 5.54 | 5.87 | .32 |

**Table 6**: Calculated Species in Water Phase in Ohaaki deep Wells and Mahanagdong MG-9D

| Well | t °C | pH | Total S Mol/kg | Total $HCO_3^-$ Mol/kg | pp ($H_2$) bar |
|---|---|---|---|---|---|
| BR42 | 200 | 6.9 | $1.2x10^{-3}$ | $1.1x10^{-2}$ | $1.0x10^{-1}$ |
| | 175 | 7.0 | $1.2x10^{-3}$ | $8.6x10^{-3}$ | $1.0x10^{-1}$ |
| BR48 | 200 | 6.4 | $3.1x10^{-4}$ | $1.3x10^{-2}$ | $2.0x10^{-1}$ |
| | 175 | 6.6 | $2.8x10^{-4}$ | $8.4x10^{-3}$ | $2.1x10^{-1}$ |
| BR49 | 200 | 7.2 | $3.0x10^{-4}$ | $1.6x10^{-2}$ | $1.5x10^{-1}$ |
| | 175 | 7.2 | $2.6x10^{-4}$ | $2.8x10^{-2}$ | $1.5x10^{-1}$ |
| MG9D | 200 | 3.29 | $5.5x10^{-3}$ | | $1.5x10^{-5}$ |

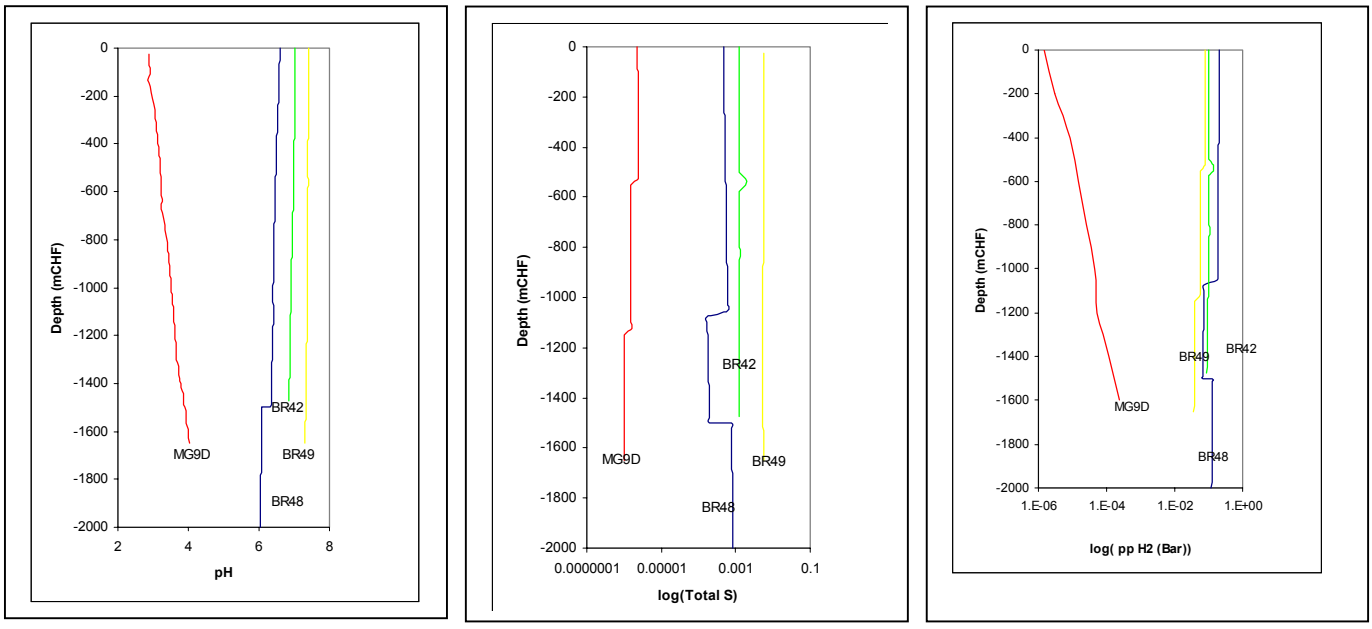


**Figure 1**: Chemical conditions in the wellbore under production conditions given in Table 3.

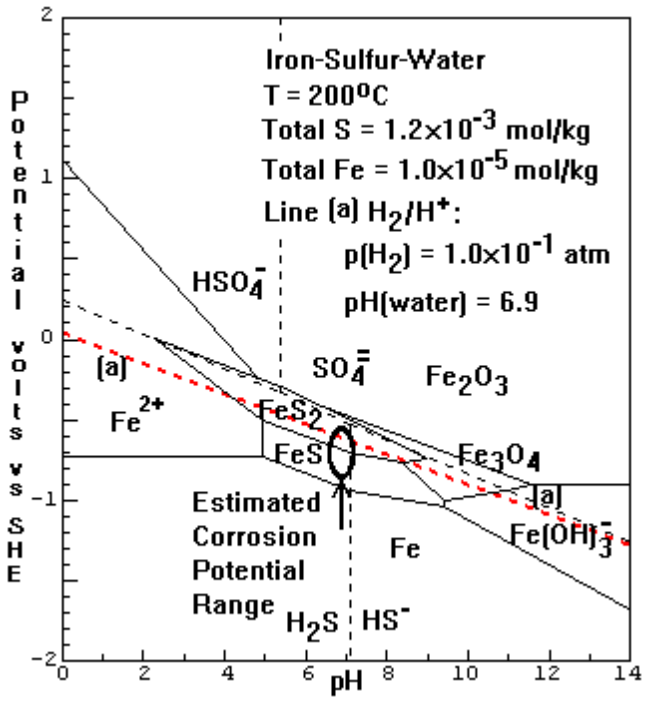


Figure 2: Potential-pH Pourbaix Diagram for Ohaaki Deep Well Water for the Fe-$H_2S$-$H_2O$ System at 200°C.

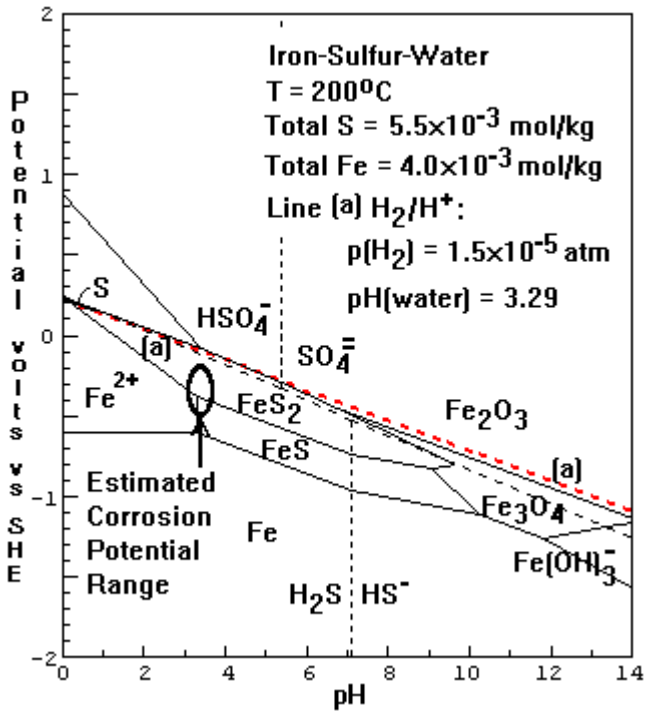


Figure 3: Potential-pH Pourbaix Diagram for Mahanagdong MG-9D Well Water for the Fe-$H_2S$-$H_2O$ System at 200°C (Lichti *et al.* 1998).